Characterisation of the decoring behaviour of inorganically bound cast-in sand cores for light metal casting

Florian Ettemeyer [a,*], Maria Schweinefuß [b], Philipp Lechner [c], Jens Stahl [c], Thomas Greß [c], Johannes Kaindl [a], Linus Durach [a], Wolfram Volk [a,c], Daniel Günther [a]

[a] *Fraunhofer Research Institution for Casting, Composite and Processing Technology IGCV, Zeppelinstraße 15, 85748, Garching, Germany*
[b] *HÜTTENES-ALBERTUS Chemische Werke GmbH, Hansastr. 1, 30419, Hannover, Germany*
[c] *Chair of Metal Forming and Casting, Technical University of Munich (TUM), Walther-Meißner-Straße 4, 85748, Garching, Germany*

1. Introduction

Due to constantly increasing requirements regarding emission reduction, the automotive industry is forced to produce highly complex components with functional integration and minimal weight. One way to produce such components is the use of casting technologies. Casting has the possibility to produce highly complex hollow structures using sand cores (Almaghariz et al., 2016). Mainly two different types of sand cores are in use. Organically bound sand cores tend to disintegrate after the casting process but also do produce harmful exhaustions. This is why more and more inorganically bound sand cores are used which mainly exhaust water. Disadvantage of inorganically bound sand cores is the relatively high residual strength after the casting process. Sand cores have opposing requirements: they need a high strength for handling operations with robots at the beginning of the casting process, e.g. for the transportation from the core blowing machine to the stock or for the placement in the casting mould. In contrast to that, the sand cores should have a low strength at the end of the casting process chain when the casting parts have to be decored. The decoring behaviour of sand cores is characterised in the literature according to Flemming and Tilch (1993) with several influencing factors like e.g the used type and amount of binder, the used sand-binder system, and casting conditions. In this study, these factors are checked and a method to sum up all influencing factors to a single parameter to describe the decoring behaviour shall be presented.

The structure of this article is stringent divided into the single methods and results due to the long process chain from specimen preparation to the decoring experiments with different routines. Section 2 prepares the state of the art of sand-binder systems and decoring characterisation. The materials and methods applied along the process chain to characterise specific properties of sand-binder systems are described in section 3. The result of each method is presented in section 4. In section 5 the single results from section 4 are discussed vice-versa, proved on correlations and put together for a deeper understanding of

* Corresponding author.
E-mail address: florian.ettemeyer@igcv.fraunhofer.de (F. Ettemeyer).

the occurring effects along the whole casting process chain.

2. State of the art

2.1. Sand cores for casting

There are mainly two different approaches to produce sand cores in industry. The most common approach is the use of a core blowing process. A mixture of sand and binder is blown into a cavity by pressured air where it is hardened thermally or chemically (Polzin, 2014). A second approach to produce sand cores is the use of a powder-based 3D-printing method where a binder system is printed onto a sand bed (Snelling et al., 2019).

2.2. Industrial decoring process

To use the hollow structures of the casting part the cast-in sand cores have to be removed after the casting process. This process is called decoring. There are several approaches to remove sand cores. Konzack (2013) proposes a method for shock wave decoring and Wolf and Polzin (2016) propose a method for decoring with pressurised air. Most common is the decoring by hammering and shaking (Stauder et al., 2018). The latter method is mainly based on mechanical impulses onto the casting part by a hammering system. The casting part is clamped and mechanical impulses onto the casting part by a pneumatic hammer (Omler srl, Bandito, Italy) induce the mechanical energy for decoring during the decoring process.

2.3. Factors influencing the decoring behaviour

According to Dietert (1950) the decoring behaviour is mainly influenced by the design of the cast component, the sand-binder system, and the hardening of the cores. Further influencing factors are the decoring method and the temperature regime on the cores due to the casting process. Flemming and Tilch (1993) also describe these basic factors and additionally mention the shrinkage of the casting part onto the sand core and more specific effects like chemical surface reactions or the gas atmosphere in the mould.

2.4. Laboratory methods to characterise the decoring behaviour

Dietert (1950) proposed as early as 1950 to measure the residual strengths of temperature treated sand cores to characterise the decoring behaviour of different sand-binder systems in a laboratory. This method is applied by many others like e.g. Kossien (2018) who postulates that beyond the casting temperature there have to be other influencing factors than the residual strength to the decoring behaviour. Further methods with cast-in specimens to characterise the decoring behaviour are mentioned by Stauder et al. (2018) with a shaking test rig or by Izdebska-Szanda et al. (2012) with a knock-out-test. Both methods measure the amount of energy necessary to decore a specimen. Major-Gabryś et al. (2014) postulate that the expansion behaviour of the sand-binder system has to be considered to characterise the decoring behaviour. A laboratory method to measure the disintegration of sand cores is described by Deters et al. (2015). Bending bars are used as specimen. The 3-point bending strength of the specimen is measured before and after a heat treatment of 400 °C for 3 min. The specimen is weighed and afterwards put on a shaker. The shaker works with a frequency of 100 s^{-1} for 60 s. In this step, the heat-treated sand core begins to disintegrate. After shaking, the solid fragments of the specimen are weighed again and with the difference of the weight before and after shaking the disintegration is determined.

2.5. Mechanics of porous media: Drucker-Prager yield criterion

There are different approaches to describe the mechanical behaviour of porous media in literature. Stauder et al. (2019) and Lechner et al. (2021) describe the mechanical behaviour by the use of a Mohr-Coulombcriterion. Thorborg et al. (2020) and Galles and Beckermann (2015) use a Drucker-Prager yield criterion to describe the mechanical behaviour of sand cores. Both criterions have in common that they describe the porous media as hydrostatic-pressure dependent in contrast to yield criterions for metals like Mises (1913) or Tresca (Matsuoka and Nakai, 1985). This means that the sand cores withstand a higher amount of strength the higher they are compressed hydrostatically. The Drucker-Prager yield criterion has a smoother yield surface in comparison to the Mohr-Coulomb model and has some numerical advantages as it does not show numerical discontinuities. For this reason the authors focus on the Drucker-Prager yield criterion, the so-called DP model, in this context. Originally intended for modelling soil, it was later expanded for the use on stone, concrete, and other materials (Öztekin et al., 2016). The DP model is also in use for modelling of low temperature creep of high strength bearing steels (Alfredsson et al., 2016).

The DP model maps the failure - more specifically the beginning of plastic flow - of a material. The basic equation is (Drucker and Prager, 1952):

$$f(I_1, J_2) = \alpha I_1 + \sqrt{J_2} - k = 0 \tag{3.1}$$

The parameters α and k are positively defined material constants, which reflect the properties of the respective material with respect to the DP model and are determined experimentally.

I_1 is the first invariant of the stress tensor and J_2 is the second invariant of the deviatoric part of the stress tensor. According to Yi et al. (2005) failure occurs when

$$f(I_1, J_2) \leq 0 \tag{3.2}$$

In Fig. 1 the DP model is depicted in the p–q plane. On the ordinate the Mises comparative stress q (also: shape change energy hypothesis) is plotted and on the abscissa the hydrostatic pressure p is plotted.

In p–q space, the DP model is a rising straight line (shear failure line), the q-axis section of which is referred to as cohesion d and the slope β as the angle of internal friction.

The linear elastic range in which Hooke's generalized law applies is below the failure line. Stress states in this area do not lead to failure. If the load reaches or exceeds the straight line, the component begins to deform plastically and a failure occurs.

The failure line can be determined experimentally by mechanical tests like the 3-point bending and the uniaxial compression test which are depicted schematically in Fig. 2.

$$\sigma_{3PB} = \frac{3Fl_{3P}}{2w_{3P}h_{3P}^2} \tag{3.3}$$

The resulting stress for 3-point bending σ_{3PB} can be calculated according to Eq. 3.3 (Assmann and Selke, 2004), whereas F is the maximum force, L_{3P} is the distance between the two supports, h_{3P} is the height, and w_{3P} the width of the specimen.

To transform the 3-point bending stress σ_{3PB} to the p–q plane (Mazel et al., 2014) the p_{3PB} and q_{3PB} stress components can be calculated according to Eq. 3.4 and Eq. 3.5:

$$p_{3PB} = -\frac{\sigma_{3PB}}{3} \tag{3.4}$$

$$q_{3PB} = \sigma_{3PB} \tag{3.5}$$

The 3-point bending test leads to a stress tensor with a state of tension with negative hydrostatic pressure component.

The resulting stress for uniaxial compression test can be calculated by Eq. 3.6 whereby F is the maximum compression force and a and b are the length and the width of the specimen (Behrens et al., 2016):

$$\sigma_{UC} = \frac{F}{t_{UC} \cdot w_{UC}} \tag{3.6}$$

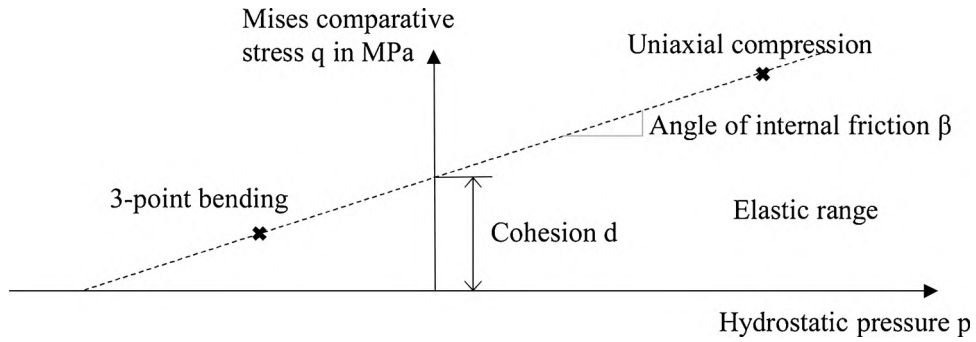

Fig. 1. Drucker-Prager yield criterion with parameters in p-q plane.

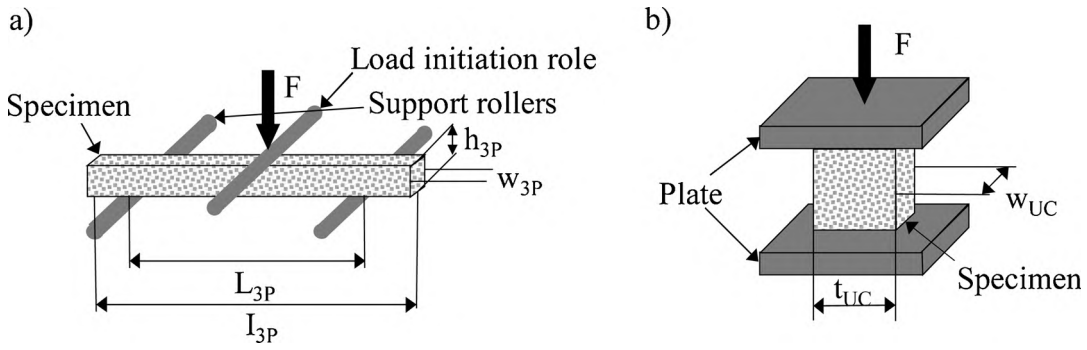

Fig. 2. Scheme of the 3-point bending a) and uniaxial compression test b).

The stress components p_{UC} and q_{UC} can be calculated according to Eq. 3.7 and Eq. 3.8:

$$p_{UC} = \frac{\sigma_{UC}}{3} \tag{3.7}$$

$$q_{UC} = \sigma_{UC} \tag{3.8}$$

2.6. Aim of the approach

Regarding the process chain of the foundry industry, see Fig. 3, it is discernible that the decoring process has many previous steps and is placed at the end of the casting process chain. Due to added value along the process chain between sand core production and the decoring process it is necessary to understand the influences of the sand-binder system to the decoring behaviour itself.

The test methods decribed in the state of the art are currently designed to measure the characteristic values of organically bound moulding materials. The new environmentally friendly inorganic binders can only be characterised inadequately. In addition, the methods can only be used in comparison, since they do not provide any material data that can be used in a simulation. This article presents a method that can be used to provide characteristic values for virtual application.

3. Materials and methods

3.1. Design of the study

The decoring behaviour of inorganically bound cast-in sand cores for light metal casting is characterised in this study. Therefore, different inorganically bound sand cores are compared both to their mechanical properties and their decoring behaviour. The decoring process is essential from an economic point of view since the decoring process needs to fit to the cycle time at the end of the process chain. Thus, it is essential to design the sand-binder system in an early state of the process.

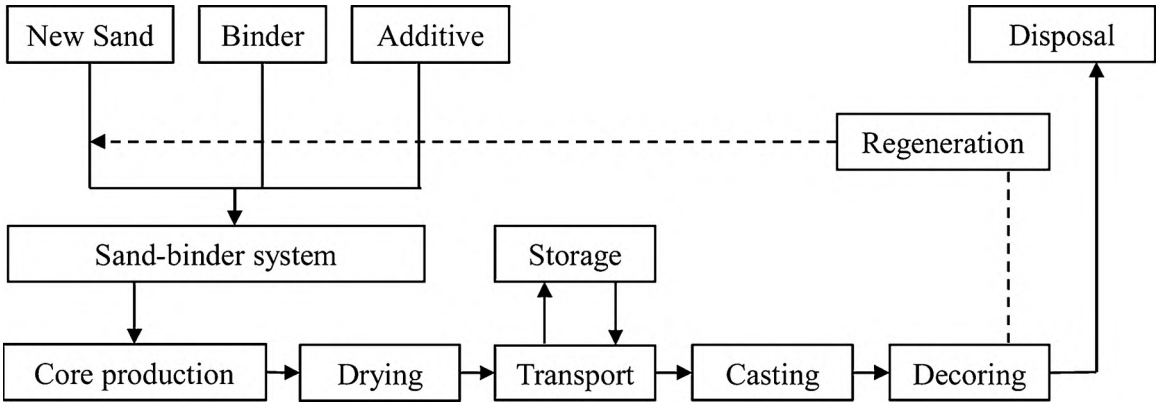

Fig. 3. Process chain of the foundry industry according to Sobczyk (2008).

Five different sand core systems (A–E) with various sand-binder mixtures are in use for this study. Both, different binder components and different sands are used. Cordis® binders are inorganic binders based on alkali silicate solutions. The model binder 1 is characterised by a high silicate-to-alkali ratio and the model binder 2 by a low silicate-to-alkali ratio. Both binders have the same solid content. The sands differ in particular in their grain shape, grain size distribution, and in their chemical composition. In Table 1 all five compared systems are shown.

System A is called reference system and has a 3-point bending strength of 2.6 MPa. The systems B–D are fit to the same 3-point bending strength like the reference system by varying the amount of binder. System E has the same amount of binder as reference system A and thus not the same bending strength as the systems A–D. With all five sand-binder mixtures sand cores are produced in the shape of bending bars as described in section 3.2 and cast-in. A mechanical material characterisation of the sand cores before and after a heat treatment was performed with state of the art measurement methods as described in the sections 3.3 and 3.4. Decoring experiments were performed on a newly developed decoring test rig and the decoring results were compared with correlations of state of the art techniques. Furthermore, the state of the art techniques for organically bound sand-binder systems shall be discussed with regard to their transferability to inorganically bound sand-binder systems.

3.2. Specimen production

All sand cores are produced in a hot-box core blowing process on a Morek LUT-1 core blowing machine (MULTISERW-Morek, Brzeźnica, Poland) with a shooting pressure of 4 bar and a shooting time of 3 s. Cavity and gassing temperature is set to 180 °C with a gassing pressure of 2 bar for 30 s.

The sand cores have the shape of a bar with a dimension of 22.4 mm x 22.4 mm x 185 mm. This type of specimen is widely used for mechanical testing of sand cores and used in many scientific investigations as shown in (Stauder et al., 2016) and (Lechner et al., 2018).

All sand bars are stored in a Memmert HPP260 climate chamber (Memmert GmbH + Co. KG, Schwabach, Germany) at 20 °C and 10 % rel. humidity to ensure constant storage conditions for the inorganically bound sand cores with hygroscopic behaviour. The aluminium specimens are produced by casting-in the sand cores in a casting mould. The process chain from sand core to aluminium specimen production is depicted in Fig. 4.

12 test specimens can be produced with one casting mould. The specimens have the shape of a hollow cuboid with a length of 150 mm and a cross-section of 42.2 mm. This means that the wall thickness of the casting part is 10 mm. For the casting part an aluminium alloy AlSi7Mg is used. Casting temperature was around 750 °C for all specimens. After cooling the casting parts are stored for 24 h in a Memmert HPP260 climate chamber at 20 °C and 10 % rel. humidity.

3.3. Measurement of mechanical properties of sand cores

3-point bending tests and compression tests were performed to determine mechanical properties for the inorganically bound sand cores. All mechanical tests were performed on an universal testing machine Zwick Z020 (ZwickRoell GmbH & Co. KG, Ulm, Germany) with a maximum tensile and compression force of 20 kN.

The 3-point bending tests are started with 3 mm min^{-1} until a preload of 0.3 N is reached. Then, the velocity is increased to 5 mm min^{-1}. The test is stopped when a force shutdown threshold of 90 % of the maximum force is reached.

The compression tests were performed with a preload of 1 N and a velocity of 5 mm min^{-1}. After reaching the preload, a testing speed of 10 mm min^{-1} was programmed. Measurement was stopped when the force reached a shutdown threshold of 80 % of the maxium compression force.

The maximum measured force is used for calculating stresses for both the bending and the compression strength. For the 3-point bending experiments only specimens with fracture in the middle and for the compression tests only specimens with flat fracture surface through the whole specimen were defined as valid and used for interpretation in this article. In Fig. 5 the fracture images that were defined as valid are depicted for the 3-point bending and the uniaxial compression test.

The mechanical properties were measured for raw sand cores and in comparison to that after a heat treatment of 400 °C for 3 min in a Nabertherm LE 14/11/R7 furnace (Nabertherm GmbH, Lilienthal, Germany) according to the specimen preparation of the disintegration test described in section 2.4.

Furthermore, for the three selected systems A, B and D mechanical properties of the cast-in sand cores were measured. Therefore, the specimens were exposed by milling the aluminium specimen with a milling machine.

The preparation of the specimens for the mechanical investigations is depicted in Fig. 6. In the first step 3-point bending tests are performed, see Fig. 6b. The resulting two fragments of the sand core are in turn cut into pieces with a width of 20 mm (Fig. 6c) and then used for a compression test. This method is performed for specimens in raw condition and in the same way for the heat treated and cast-in specimens.

All measured maximum forces were transformed into a stress-state as described in section 2.5.

3.4. Measurement of casting shrinkage

Strain gauges are applied to the casting part at two positions and the sand core is drilled out by a drilling machine, see Fig. 7, to determine the shrinkage of the casting part onto the cast-in sand core. The releasing strains of the aluminium part due to the removed sand core are measured by a HBM QuantumX MX840B universal measuring amplifier.

The strain gauges are applied at two different positions and the strains are measured in x- and y-directions. The induced stress onto the sand core for the cast-in specimen can be calculated with the released strain by drilling-out the sand core. The measured strains are expected to be representative not only in the x–y plane but also in the other four walls of the specimen due to the symmetric structure of the specimen.

3.5. Decoring of the specimens

Starting from the industrial decoring process a mechanical test rig for decoring experiments is derived. The developed test rig for investigating

Table 1
Composition of the investigated sand cores; a HA Anorgit(R) powder additive was used in all mixtures with a binder:additive ratio of 2.68:1.

System	A	B	C	D	E
Raw material	Silica sand H32	Silica sand H32	Bauxit W65	Silica sand F34	Silica sand F34
Amount of binder in wt%	1.9	1.5	0.75	2.25	1.9
Type of binder (HA Cordis®-model binder)	1	2	1	1	1
Variation	Reference system	Binder	Grain shape and grain size distribution	Grain size distribution	Same amount of binder like reference system A, but different grain size distribution

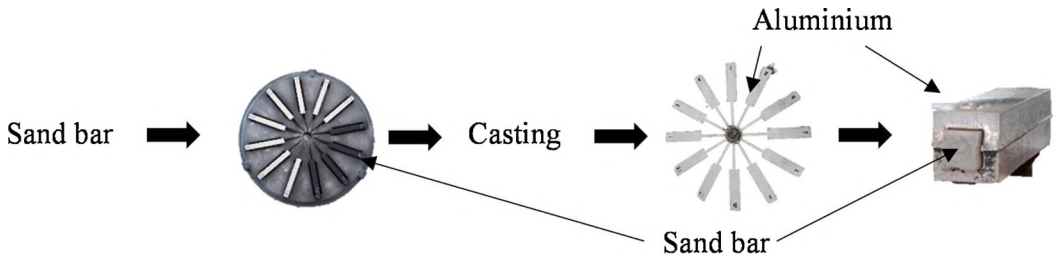

Fig. 4. Process chain to manufacture specimens for experimental investigations.

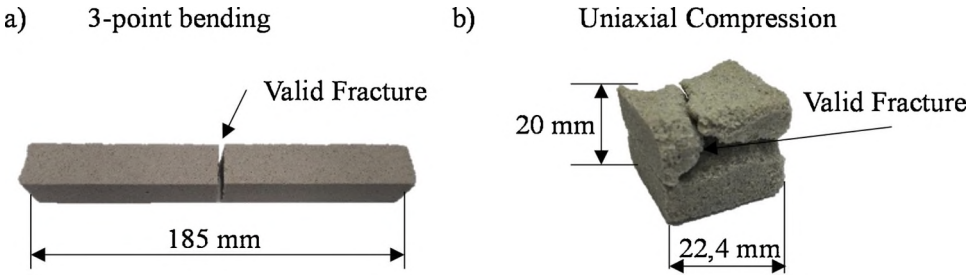

Fig. 5. Visualisation of valid fracture behaviour for 3-point bending and uniaxial compression test.

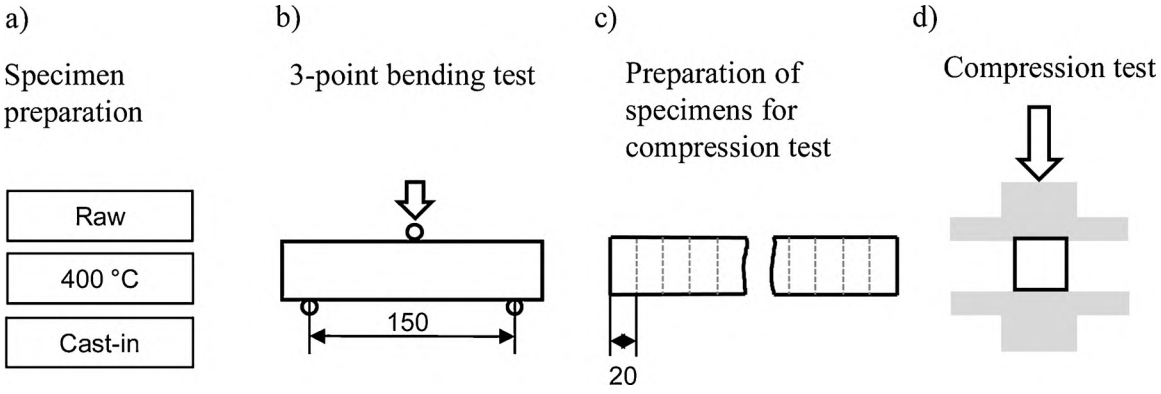

Fig. 6. Method of specimen preparation.

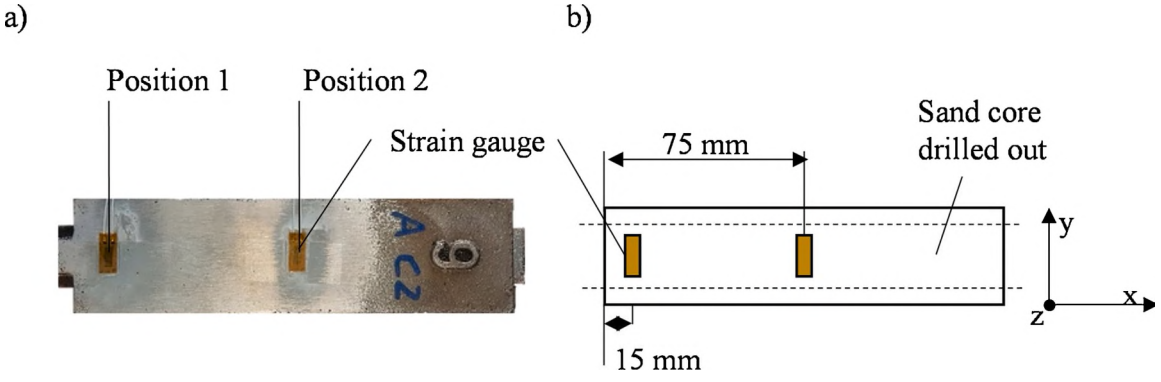

Fig. 7. Method to measure the shrinkage of the casting part onto the cast-in sand core in x- and y-direction.

the decoring behaviour is depicted in Fig. 8.

A ram weight can be manually lifted using a crank. From the highest position the ram weight falls down by a free fall and induces an impulse depending on the ram weight and the fall height onto the clamped casting part. A spring mechanism is installed which locks the ram after the first spring-back from the casting part to ensure that the ram does not induce more than one impulse per crank round.

The energy level for decoring is set in a way that the reference system A, see Table 1, is decored completely within 100 impulses. Therefore, the weight of the ram is set to 6.8 kg and the fall height of the ram is set to 50 mm which leads to an energy of 3.3 Joules per impact. During the experiments the velocity and the acceleration of the specimen were measured by a laser vibrometer Polytec CLV-2534 (Polytec GmbH, Waldbronn, Germany) and all data were recorded by a HBM QuantumX

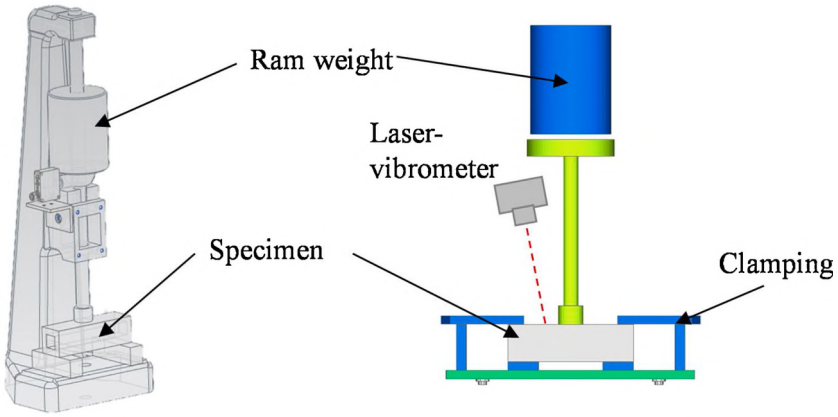

Fig. 8. Scheme of the new developed test rig for investigating the decoring behaviour derived from the industrial state of the art.

MX840B universal measuring amplifier with a sampling rate of 38,500 s^{-1} (Hottinger Baldwin Messtechnik GmbH, Darmstadt, Germany).

At the beginning and after every 20 impacts the weight of the casting part with the cast-in sand core is measured to determine the decoring effort. Furthermore, at the beginning and after every 20 impacts the decoring depth of the sand core is measured on both sides of the casting specimen with a measuring stick. The specimen is defined as decored when the sand core is removed completely.

4. Experimental results

4.1. Measurement of mechanical properties of sand cores

The results of the 3-point bending and the compression tests for the raw sand cores, the sand cores after the heat treatment at 400 °C for 3 min, and for the cast-in sand cores for all five recipes are depicted graphically in Fig. 9.

The systems A–D were fit to the same bending strength of 2.6 MPa by varying the amount of binder. With a standard deviation of 0.2 MPa this is in a good range. System E is not adjusted to the bending strength of reference system A but to the same amount of binder like system A. This leads to a lower bending strength of 2.2 MPa. This effect can be explained by the finer grain size distribution of silica sand F34 of system E in comparison with the coarser silica sand H32 of reference system A. The compressive strengths of the systems A and D in raw condition have a similar strength level between 9.6 MPa and 9.1 MPa, respectively. Both systems do have a higher compression strength compared to the remaining systems B, C and E which show values between 7.4 MPa and 6.6 MPa. A clear differentiation of the systems regarding the compressive strength is not possible at this stage since the standard deviations of the experimental results overlap to a high amount between systems A and D and B, C, and E, respectively for the raw specimens. This effect can be explained by the more complex border conditions of the compression test in contrast to bending tests which can lead to higher standard deviations in the results as is shown in this results.

The heat treated specimens with a heat exposure of 400 °C for three minutes show in general a decrease of bending and compression strength compared with the raw specimens. The bending strength decreases to maximum values of 1.5 MPa for the systems A and D and minimum strengths of 1 MPa for the systems B and E. System C decreases to a bending strength of 1.2 MPa. Generally, no clear differentiation of the bending strengths is possible. The compression strength distributes between 5.3 MPa for system C and 8.5 MPa for system D. The standard deviations of the results increase in particular for the compression tests. The standard deviations of the three-point bending tests do not seem to be affected due to the heat treatment in general.

The measured strengths of the cast-in sand cores for the systems A, B and D show a significant and strong decrease compared with raw and heat-treated specimens. This strong decrease in strength is clearly visible comparing Fig. 9a, b, and c. Whereas the bending strengths of the systems vary between 0.1 MPa for system A and B and 0.2 MPa for system D, the compression strengths vary between 0.1 MPa for system B, 0.2 MPa for system A and 0.5 MPa for system D, respectively. Please note the scaling of the abscissa which shows a decrease by factor 30 compared to the initial strengths.

4.2. Measurement of the disintegration

The results of the disintegration investigations according to section 2.4 are shown in Table 2.

The higher the value of the disintegration (=sieve through fraction), the easier the decoring behaviour of the specimen is expected. The disintegration measurements show the highest value of 67 % for system B which was produced with binder type 2. System C with base material Bauxit W65 and system A and E with base material silica sand seem to have a similar disintegration. For system D, the lowest value of disintegration was measured.

4.3. Casting shrinkage

The results of the measured strains are shown in Table 3. Values without specified standard deviations derive from single measurements.

The negative sign of the values means a shrinkage of the aluminium casting part due to the removal of the sand core. This means that the cast-in sand cores are under pressure after the casting and before the decoring process. This is due to the shrinkage of the casting part onto the sand core during the cooling process. The absolute values for specimen A with H32 silica-sand as base material and specimen D with F34 silica-sand are 120 μm/m for position 1 and 185–200 μm/m for position 2 at the same magnitude. Please note that for system C no values could be measured due to self-decoring of the system after casting.

4.4. Measurement of the decoring behaviour

The cast-in sand cores were decored on the single-impulse decoring test rig described in section 3.5. The number of impacts until complete decoring is tabulated in Table 4. It can be seen that system A needs on average 99 impulses to get completely decored, which fits in a good manner the requirement of chapter 3.5 to be decored within 100 impulses. System B is decored within about 20 impulses and thus decored five times faster than system A. System C could not be measured on the decoring test rig due to the fact that the sand cores of system C completely fell apart directly during unpacking from the casting mould. System D has an average need of 229 impacts to be fully decored. This means that system D needs more than two times more single impacts to get decored in comparison to reference system A although both systems

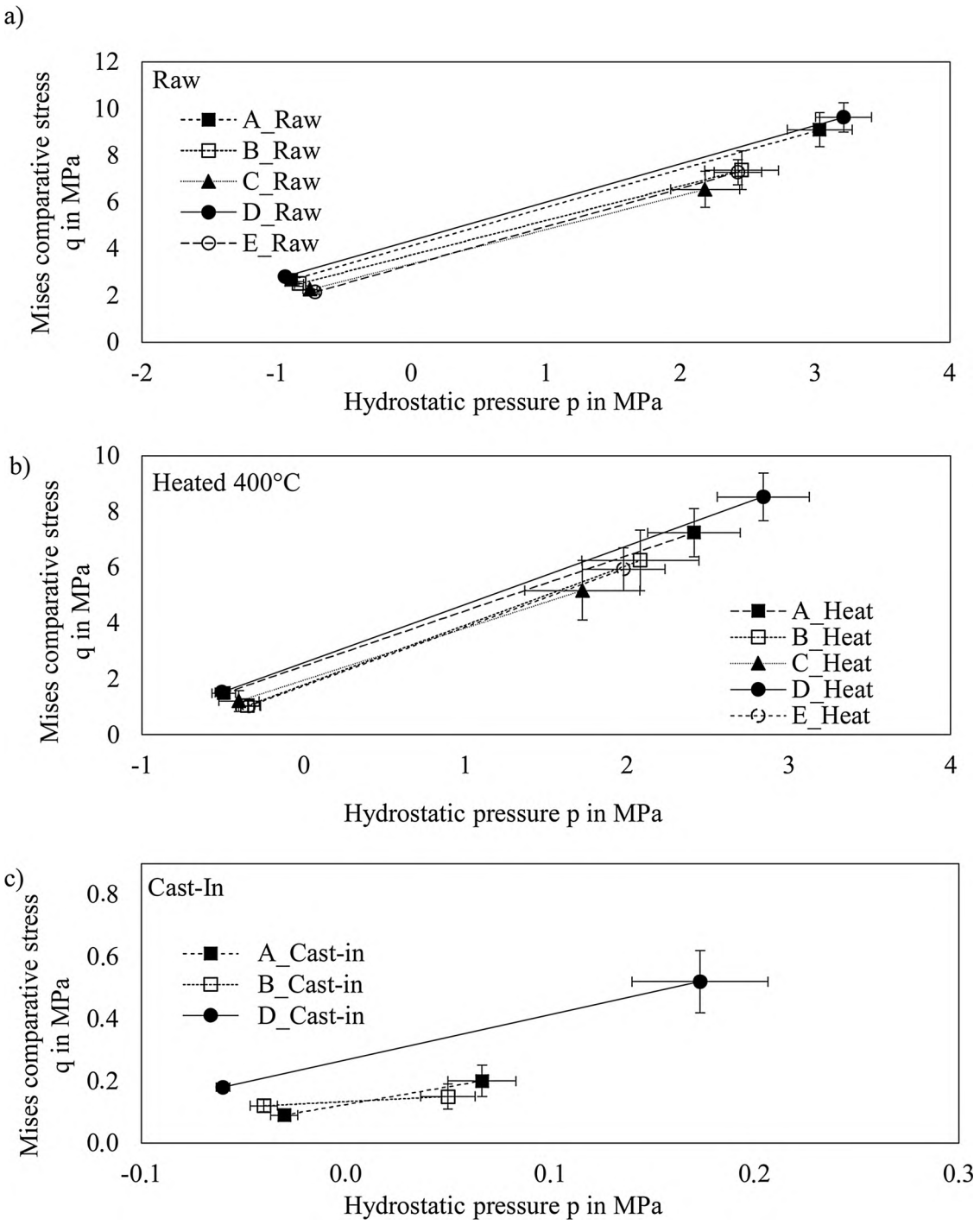

Fig. 9. Results of the mechanical properties of raw a) heat treated b) and cast-in c) sand cores in a p-q diagram.

Table 2
Results of the disintegration measurements according to section 2.4

System	A	B	C	D	E
Disintegration in %	45 ± 2	67 ± 3	48 ± 1	28 ± 0	42 ± 3

had the same mechanical strength in raw condition. System E can be decored after 70 impacts and therefore is decored faster than reference system A although the same amount of binder was used to produce the specimens of both systems. All sand cores are decored from the open side of the specimen to the middle. No fracture in the middle of the sand cores due to bending impulses could be detected.

Table 3
Results of strain measurements for drilled-out specimens.

Position	System	A	D
Position 1	Measured strain x-direction µm/m	No value measured	No value measured
	Measured strain y-direction in µm/m	−120	−120
Position 2	Measured strain x-direction µm/m	−25	No value measured
	Measured strain y-direction µm/m	−185 ± 21 (2 measurements)	−200 ± 10 (3 measurements)

Table 4
Decoring behaviour of the five investigated specimen systems.

System	A	B	C	D	E
Amount of specimens tested	44	12	24	16	36
Number of impacts until decoring	99 ± 24	17 ± 7	0 ± 0	229 ± 82	70 ± 23
Number of impacts until decoring with standard deviation in %	99 ± 24	17 ± 41	0 ± 0	229 ± 35	70 ± 33

5. Discussion

5.1. Methods and properties of sand cores

In general, all experimental data show a big spread of the results with standard deviations up to maximum 41 % for the decoring behaviour of system B. The high standard deviations occur already for the freshly produced sand cores and are a well-known phenomenon in the use of inorganically bound sand cores. The error bars in the experimental results can spread further due to the long process chain from core production to the measurement of the decoring behaviour including casting and storage in the climate chamber. This effect is well-known in literature and described, e.g. in Stauder et al. (2018) for core removal of silicate bonded sand. Nevertheless, the investigated systems show a clear trend and can be distinguished in their decoring behaviour.

5.2. Correlation between the amount of binder and decoring behaviour

Regarding the used amount of binder in the production process of the sand cores according to Table 1 a clear correlation between decoring behaviour and amount of binder can be seen for systems A to D. For these four systems a correlation between binder and decoring behaviour could be found. One would assume that a higher amount of binder leads to a worse decoring behaviour. This finding is also described in literature by Stauder (2018). Considering system E with the same amount of binder like system A, this finding shows that the binder amount is not the only decisive factor for the decoring behaviour. The correlation between the number of impacts until complete decoring and the amount of binder used for core production is depicted in Fig. 10. It should be noted, that the amount of binder is defined for core production and therefore no standard deviation and no numbers of values measured can be mentioned.

5.3. Correlation of the decoring behaviour with results from disintegration test

The number of impacts until complete decoring are depicted in Fig. 11 in comparison to the results from the disintegration test.

The results of the disintegration test are scaled to reference system A in order to compare the results in a simple way. Due to the fact that a higher value of disintegration would imply a better decoring behaviour, consequently a lower number of needed impacts until decoring would be expected. One can see that this inverse correlation is correct for systems A, B, and D. For system C, from the value of disintegration one would expect a similar decoring behaviour like system A, which does not fit the experimental result of decoring. Furthermore, for system E a higher amount of impacts for decoring would be expected, which is not confirmed by the experimental results of the decoring test rig either. Consequently, the results show that with the disintegration method the decoring behaviour cannot be predicted properly for inorganically bound sand cores.

5.4. Shrinkage of casting part onto the sand core

The values for the shrinkage onto the casting part seem to be in the same amount for both used silica sand types. In the y-direction the shrinkage has a higher amount than in the x-direction. In the y-direction the incompressible sand system is clamped and the resulting stresses are absorbed by the sand. In the x-direction the casting part can contract and strains can for this geometry only be transmitted by friction. Hence, only small strains can be measured in the middle of the specimen on position 2 and no values could be measured at position 1. With the measured strains and Hook's law $\sigma = \varepsilon \cdot E$, which means that the stress σ can be calculated by multiplication of the strain ε and the modulus E, a rough appraisal for the resulting stress in the sand core due to shrinking of the aluminium can be calculated. A hydrostatic pressure of maximum 6 MPa can be calculated by adoption of a modulus of about 3.5 GPa for heated sand cores (Stauder et al., 2019). The amount of the hydrostatic pressure is much higher than the measured compression and bending strengths for the sand cores and shows the need for a pressure-dependent material model like the Drucker-Prager criterion.

5.5. Correlation of mechanical characteristics with decoring behaviour

The systems A–D were set to an initial middle 3-point-bending strength of 2.6 MPa by varying the amount of binder in sand core production. The experimental average of the specimens A–D is with a value of 2.6 MPa and a standard deviation of 0.2 MPa in a good range.

The bending strength is decreasing more than the compression strength regarding the heat treated sand bars. The compression

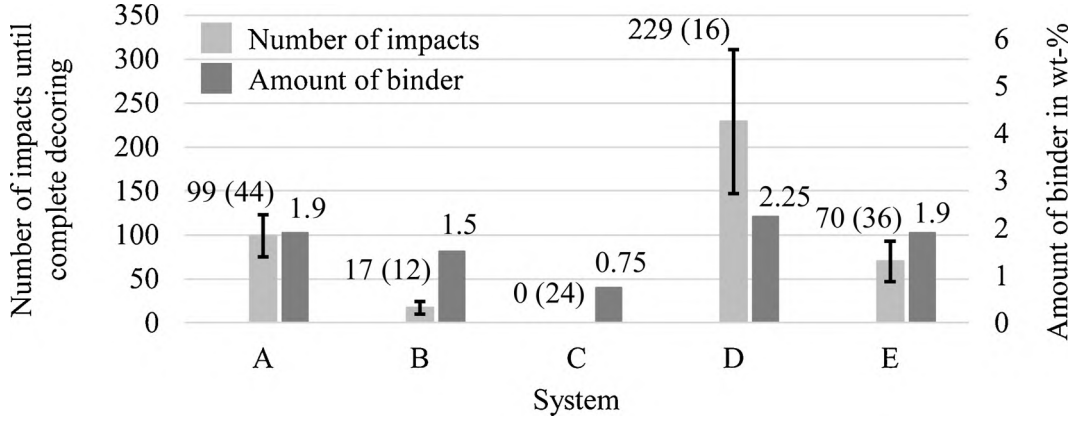

Fig. 10. Visualisation of the correlation between the number of impacts until complete decoring and the amount of binder used for core production. The number of specimens tested is mentioned in brackets.

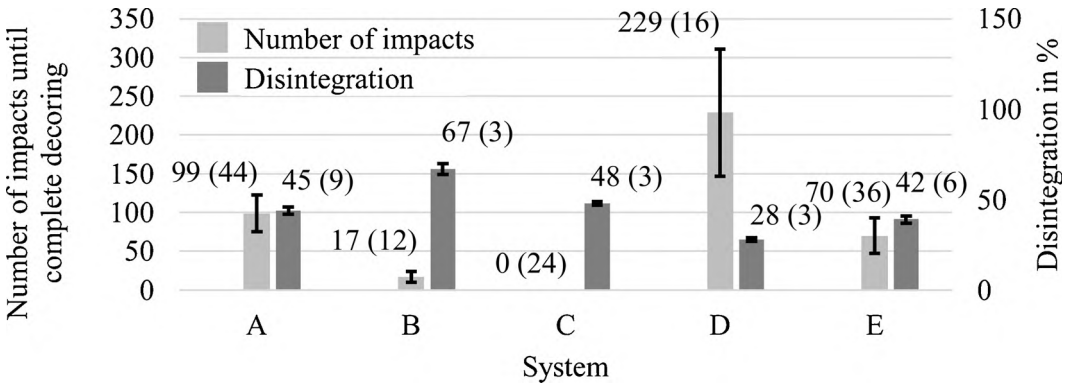

Fig. 11. Visualisation of the correlation between the number of impacts until complete decoring and results of disintegration measurements. The number of specimens tested is mentioned in brackets.

strengths, both for raw and heated sand cores, show a bigger spread than the 3-point bending strengths. The middle values of the compression strengths tend to show higher differences after heat exposure. The bigger spread of the compression strengths is explained by the influence of the sand microstructure. Whereas the systems A, B, D and E do have silica sand as a base material, system C has Bauxit W65 sand as a base material, which has a rounder shape (Ettemeyer et al., 2020). The bigger spread of the standard deviations can be explained by the more complex support conditions for the uniaxial compression test. The contact surface between the sand core and testing equipment for the compression test is a flat support and therefore more sensitive to roughnesses compared to the line support for 3-point bending tests. Especially for granular media like sand cores, which tend to break under shear fracture, this factor can have a high influence.

No clear correlation of the decoring behaviour and the mechanical properties of heat treated specimens after an exposure at 400 °C for three minutes can be detected due to big error bars. Especially the decoring behaviour of system B and system E cannot be correlated with the measured compression strengths.

Regarding the cast-in and milled out specimens A, B, and D no correlation of the bending strength and the decoring behaviour can be found, see Fig. 9. For system C no mechanical properties are measured due to self-decoring after the casting. The measured compression strengths of the remaining systems themselves show a weak correlation for their middle values. Nevertheless, a clear correlation is difficult to prove due to the error bars. Regarding the angle of friction for the three characteristic systems, a correlation can be found with no overlapping error bars. A comparison of the angle of friction for cast-in sand cores and the number of needed impacts for decoring is depicted in Fig. 12

The influence of the angle of friction and the compression stress to the decoring behaviour can also be explained by use of simulation.

5.6. Simulation

To understand the influence of the hydrostatically pressure-dependent material model in a deeper way, a simulation of the decoring setup is modelled. The material parameters for the alminium specimen and the sand core were adapted from Ettemeyer et al. (2018) and are provided in Table 5.

The simulation is set up in the simulation software Abaqus (Dassault Systèmes, Vélizy-Villacoublay Cedex, France) without a yield criterion and calculating linear elastic. All stress tensors are calculated linear elastic for every time-step in the simulation. The stress matrices are calculated to the von Mises stress component q and the hydrostatic pressure component p according to Fig. 1 with the software Matlab (MathWorks, 1 Apple Hill Drive, USA) in a postprocessing step. In Fig. 13 the simulated decoring behaviour is depicted graphically. Every square in the diagram in Fig. 13a represents an element of the cast-in sand core. Elements above the Drucker-Prager failure line are expected to be destroyed and marked black in Fig. 13b for a friction angle of 50° and in Fig. 13c for an internal friction angle of 30°, respectively.

The failure lines are both set to the same 3-point bending strength and to different compression strengths. This matches the experimental results described in chapter 5.1 where the sand cores show differences in the compression strengths with similar 3-point bending strengths.

Table 5
Material parameters for simulation according to Ettemeyer et al. (2018).

Parameter	Youngs Modulus in GPa	Density in kg m^{-3}	Poisson's ratio
Aluminium AlSi7Mg	70	2700	0.3
Sand core	7	1600	0.3

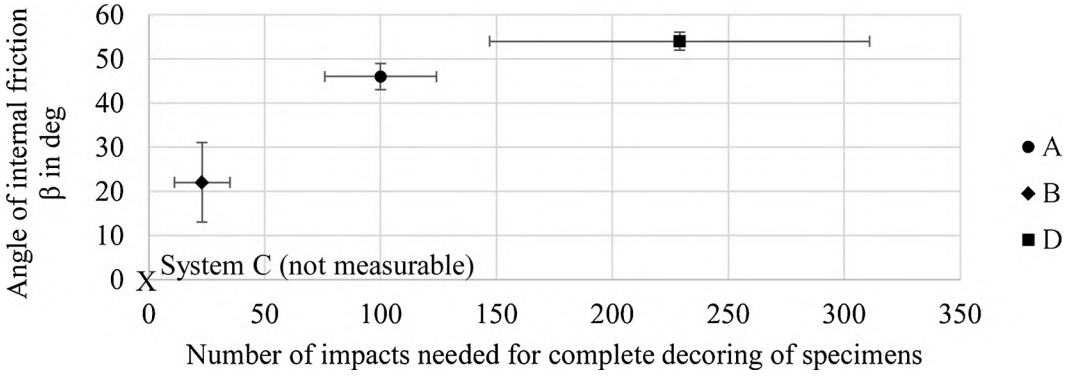

Fig. 12. Angle of friction of cast-in sand cores correlated with number of needed impacts for decoring.

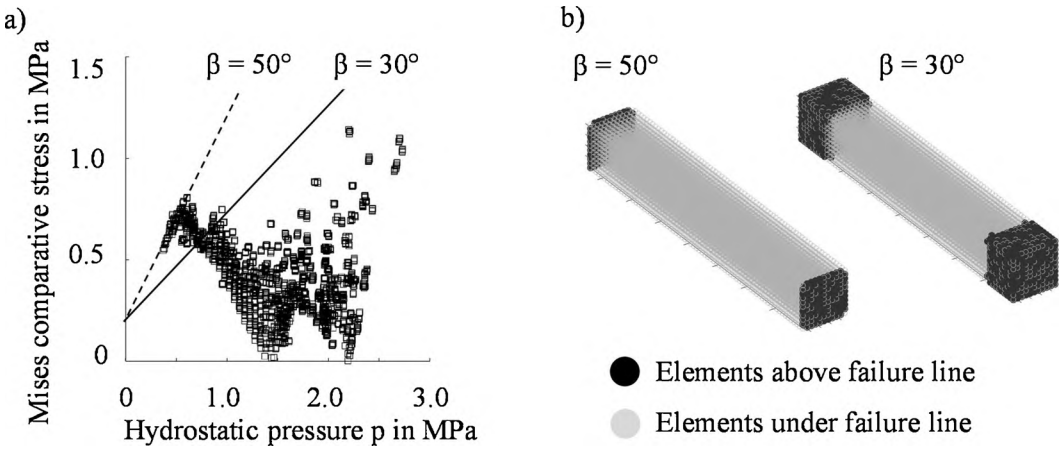

Fig. 13. Results from qualitative stress-state for sand specimen with the same 3-point bending strength and varying compression strengths.

It is discernible that with higher compression strength (Fig. 13b) less elements are destroyed which means that the core needs more impacts to get destroyed. On the other hand sand cores with a lower compression strength tend to be decored after fewer impacts. This finding means that not only the amount of used binder is significant for the development of sand-binder systems with good decoring properties but also the shape and the sieve-line of the base moulding material. For a good decoring behaviour the use of a material with low friction angles and low bending and compression strengths after heat indication in general are recommended.

This finding can be important for further investigations because it confirms the validity of a pressure-dependent material behaviour. The possibility to describe the behaviour of the decoring of cast-in sand cores with such a pressure-dependent material model is a relevant task for industry to save resources and to understand and predict the decoring process.

6. Conclusion

A new measuring method for the decoring process of cast-in sand cores which describes the decoring process more directly than classic investigations in the laboratory is introduced in this article. The measuring method was adapted from the industrial state of the art. Five different inorganically bound sand-binder systems were investigated within this study and compared regarding their mechanical properties. A Drucker-Prager yield criterion was adapted to describe the decoring behaviour and a direct correlation between the decoring behaviour and mechanical compression strength was a finding of the investigations. The method to mill out cast-in sand cores and to measure the mechanical properties of these specimens is not reported until now and is consequently new. Furthermore, the authors could show that a heat treatment of 400 °C for three minutes is not appropriate to characterise the decoring behaviour of inorganically bound sand cores. Moreover, the investigations showed that classic disintegration methods are not suitable for the investigated inorganically bound sand-binder systems. In particular, the opportunity to correlate the decoring behaviour with the internal angle of friction for inorganically bound cast-in sand cores is a new approach and allows to model new sand-binder systems with enough bending strength for handling operations and with low compression strength for a good decoring behaviour after the casting process. Consequently, the findings allow a targeted selection and development of moulding material mixtures (binder type and sand system) to optimise the decoring behaviour in highly complex casting parts. The results are planned to be adapted to industrially relevant high-complex casting parts like cylinder heads in further investigations. Moreover, the results presented in this paper all refer to the same amplitude of the hammering impact. It would be interesting to refer the decoring behaviour to variable impact amplitudes in further investigations.

CRediT authorship contribution statement

Florian Ettemeyer: Investigations, Methodology, Writing – Original Draft, Writing – Review & Editing, Project administration. **Maria Schweinefuß:** Investigations, Resources. **Philipp Lechner:** Investigations, Resources. **Jens Stahl:** Investigations, Resources. **Thomas Greß:** Investigations, Resources. **Johannes Kaindl:** Investigations, Validation. **Linus Durach:** Investigations, Simulation. **Wolfram Volk:** Supervision, Funding administration. **Daniel Günther:** Supervision, Funding administration.

Declaration of Competing Interest

The authors report no declarations of interest.

Acknowledgements

The authors would like to thank HÜTTENES-ALBERTUS Chemische Werke GmbH for providing materials for this research and FILL GmbH for providing an industrial decoring test rig. Parts of this study are financed by DFG under the grant number VO 1487/37-1and by Bavarian Ministry of Economic Affairs, Regional Development and Energy under the grant number RvS-SG20-3451-1/37/6.

The authors want to express their gratitude to Dr. rer. nat Christian Lustig and Dr.-Ing. Lukas Mirko Reinold from HÜTTENES-ALBERTUS Chemische Werke GmbH and Dipl.-Ing. Harald Sehrschön from FILL GmbH for proofreading, technical input, and support in project realisation.

References

Alfredsson, B., Arregui, I.L., Lai, J., 2016. Low temperature creep in a high strength roller bearing steel. Mech. Mater. 100, 109–125.

Almaghariz, E.S., Conner, B.P., Lenner, L., Gullapalli, R., Manogharan, G.P., Lamoncha, B., Fang, M., 2016. Quantifying the role of part design complexity in using 3D sand printing for molds and cores. Int. J. Met. 10 (3), 240–252, 2016.

Assmann, B., Selke, P., 2004. Technische Mechanik. Oldenbourg Verlag., Berlin.

Behrens, B.A., Bouguecha, A., Vucetic, M., Bonhage, M., Zaitsev, A., Malik, I.Y., 2016. Compaction of a copper spiral within a cylindrical die of steel powder and investigation of their deformation behaviour. In: European Congress and Exhibition on Powder Metallurgy. European PM Conference Proceedings. The European Powder Metallurgy Association, pp. 1–6.

Deters, H., Oberleiter, M., Zupan, H., 2015. Formstoffmischungen enthaltend eine oxidische Bor-Verbindung und Verfahren zur Herstellung von Formen und Kernen. (DE 10 2013 111 626 A1). Deutsches Patent- und Markenamt.

Dietert, H.W., 1950. Foundry Core Practice. American Foundrymen's Society, pp. 473–478.

Drucker, D.C., Prager, W., 1952. Soil mechanics and plastic analysis or limit design. Q. Appl. Math. 10 (2), 157–165.
Ettemeyer, F., Steinlehner, F., Lechner, P., Volk, W., Günther, D., 2018. Detection of core fracture in inorganically bound cast-in Sand cores by acoustic microphony. Congress of the German Academic Association for Production Technology. Springer, Cham, pp. 34–43.
Ettemeyer, F., Lechner, P., Hofmann, T., Andrä, H., Schneider, M., Grund, D., Volk, W., Günther, D., 2020. Digital sand core physics: predicting physical properties of sand cores by simulations on digital microstructures. Int. J. Solids Struct. 188-189, 155–168. https://doi.org/10.1016/j.ijsolstr.2019.09.014.
Flemming, E., Tilch, W., 1993. Formstoffe und Formverfahren: mit 118 Tabellen. Dt. Verlag für Grundstoffindustrie.
Galles, D., Beckermann, C., 2015. Effect of sand dilation on core expansion during steel casting. In: IOP Conference Series: Materials Science and Engineering 84(1). IOP Publishing.
Izdebska-Szanda, I., Angrecki, M., Matuszewski, S., 2012. Investigating of the knocking out properties of moulding sands with new inorganic binders used for castings of non-ferrous metal alloys in comparison with the previously used. Arch. Foundry Eng. 12 (2), 117–120.
Konzack, C., 2013. Entkernen von Gussprototypen mit Stoßwellen: Das Säubern von Gussteilen mit der Stoßwellentechnologie verkürzt die Produktionszeit bei ACTech deutlich. Giesserei 11, 62–63.
Kossien, B., 2018. Untersuchungen zur sekundären Verfestigung von wasserglasgebundenen Formstoffen für Eisen-und Stahlguss. Dissertation. Technische Universität Bergakademie Freiberg.
Lechner, P., Stahl, J., Ettemeyer, F., Himmel, B., Tananau-Blumenschein, B., Volk, W., 2018. Fracture statistics for inorganically-bound core materials. Materials 11 (11), 2306. https://doi.org/10.3390/ma11112306.
Lechner, P., Hartmann, C., Ettemeyer, F., Volk, W., 2021. A plane stress failure criterion for inorganically-bound core materials. Materials 14 (2), 247.
Major-Gabryś, K., Dobosz, S.M., Jelínek, P., Jakubski, J., Beňo, J., 2014. The measurement of high-temperature expansion as the standard of estimation the knock-out properties of moulding sands with hydrated sodium silicate. Arch. Metall. Mater. 59 (2) https://doi.org/10.2478/amm-2014-0123.
Matsuoka, H., Nakai, T., 1985. Relationship among tresca, mises, mohr-coulomb and matsuoka-nakai failure criteria. Soils Found. 25 (4), 123–128.
Mazel, V., Diarra, H., Busignies, V., Tchoreloff, P., 2014. Comparison of different failure tests for pharmaceutical tablets: applicability of the Drucker–prager failure criterion. Int. J. Pharm. 470 (1-2), 63–69. https://doi.org/10.1016/j.ijpharm.2014.05.006.
Mises, R.V., 1913. Mechanik der festen Körper im plastisch-deformablen Zustand. Nachrichten von der Gesellschaft der Wissenschaften zu Göttingen. Mathematisch-Physikalische Klasse, pp. 582–592, 1913.
Öztekin, E., Pul, S., Hüsem, M., 2016. Experimental determination of Drucker-Prager yield criterion parameters for normal and high strength concretes under triaxial compression. Constr. Build. Mater. 112, 725–732. https://doi.org/10.1016/j.conbuildmat.2016.02.127.
Polzin, H., 2014. Inorganic Binders: For Mould and Core Production in The Foundry. Fachverlag Schiele & Schön, Berlin.
Snelling, D.A., Williams, C.B., Druschitz, A.P., 2019. Mechanical and material properties of castings produced via 3D printed molds. Addit. Manuf. 27, 199–207.
Sobczyk, M., 2008. Untersuchung zur Nutzung der Vakuumtrocknungshärtung für die Herstellung und den Einsatz magnesiumsulfatgebundener Kerne für den Leichtmetallguss. Dissertation. Otto-von-Guericke-Universität Magdeburg.
Stauder, B.J., 2018. Investigation on the Removal of Internal Sand Cores From Aluminium Castings. Dissertation. Montanuniversität Leoben.
Stauder, B.J., Kerber, H., Schumacher, P., 2016. Foundry sand core property assessment by 3-point bending test evaluation. J. Mater. Process. Technol. 237, 188–196. https://doi.org/10.1016/j.jmatprotec.2016.06.010.
Stauder, B.J., Harmuth, H., Schumacher, P., 2018. De-agglomeration rate of silicate bonded sand cores during core removal. J. Mater. Process. Technol. 252, 652–658. https://doi.org/10.1016/j.jmatprotec.2017.10.027.
Stauder, B.J., Berbic, M., Schumacher, P., 2019. Mohr-Coulomb failure criterion from unidirectional mechanical testing of sand cores after thermal exposure. J. Mater. Process. Technol. 274, 116274 https://doi.org/10.1016/j.jmatprotec.2019.116274.
Thorborg, J., Kumar, S., Wagner, I., Sturm, J.C., 2020.). The virtual core-modelling and optimization of core manufacturing and application. In: IOP Conference Series: Materials Science and Engineering (Vol. 861, No. 1, P. 012004). IOP Publishing. https://doi.org/10.1088/1757-899X/861/1/012004.
Wolf, G., Polzin, H., 2016. *Verfahren zum Entkernen von Gussteilen mit anschließender Regenerierung des Kernaltsandes* (DE102015004889A1). Deutsches Patent- und Markenamt.
Yi, X., Valkó, P.P., Russell, J.E., 2005. Effect of rock strength criterion on the predicted onset of sand production. Int. J. Geomech. 5 (1), 66–73.